

# Investigation of the pyrolysis of lead zirconate titanate gels with coupled differential thermal analysis, thermogravimetry and infrared spectroscopy

R. MERKLE, H. BERTAGNOLLI

*Institut für Physikalische Chemie, Universität Stuttgart, Pfaffenwaldring 55, D-70550 Stuttgart, Germany*

The pyrolysis of organic components in the sol-gel preparation of lead zirconate titanate (PZT) from lead acetate and zirconium and titanium propanolate in methoxyethanol is studied with simultaneous differential thermal analysis, thermogravimetry and infrared spectroscopy. The first pyrolysis step of the dried PZT gel, yielding acetone and CO<sub>2</sub> similar to the pyrolysis of lead acetate, indicates that most of the acetate groups are bonded to Pb<sup>2+</sup>. In the second step, the remaining organic components are oxidized to CO<sub>2</sub> and H<sub>2</sub>O. The formation of undesired carbon residues during pyrolysis from unhydrolysed alkoxide groups and acetate groups bonded to Zr<sup>4+</sup> and Ti<sup>4+</sup> can be prevented by steam treatment of the dried gels. Activation energies for the different pyrolysis steps of lead, zirconium and titanium acetate, lead decanoate and PZT gels are given. © 1998 Kluwer Academic Publishers

## 1. Introduction

The first sol-gel preparation of lead zirconate titanate, PbZr<sub>x</sub>Ti<sub>1-x</sub>O<sub>3</sub> (PZT(*x*), *x* = zirconium content in per cent) was reported in 1984 [1], with lead-(2-ethylhexanoate), titanium butanolate and zirconium acetylacetonate as starting materials and *n*-butanol as solvent. The preparation commonly applied later utilizes lead acetate, titanium and zirconium alkoxides (<sup>i</sup>propoxide, <sup>n</sup>propoxide, <sup>n</sup>butoxide) in 2-methoxyethanol as solvent [2–4]. The exchange of unidentate alkoxides by methoxyethoxide from the solvent is fast, even at room temperature [5], so that most of the alkoxides are transformed to methoxyethoxides. In the gelation step, a major part of the methoxyethoxide groups is hydrolysed off. The remaining organic components of the dried PZT gel are pyrolysed by heating to 300–400 °C in air.

Pyrolysis of dried PZT gels is an important step on the way from amorphous, metallo-organic precursors to inorganic ceramic materials. A close investigation is necessary to overcome the complications in the pyrolysis, which can severely disturb the following crystallization steps. The PZT gel samples prepared in methoxyethanol often exhibit a black colour in the temperature range 250–500 °C. Thermogravimetric (TGA) and differential thermal analysis (DTA) show a strongly exothermic weight loss at 400–500 °C [3, 4, 6, 7] from combustion of the remaining organic residues. This DTA peak covers the weakly exothermic crystallization peaks and makes investigation of the crystallization kinetics by DTA impossible. Some authors even find elementary lead from the reduction

of PbO with organic residues [8–10]. This destroys the homogenous distribution of all components in the amorphous PZT, which is the aim of the sol-gel process and essential for low crystallization temperatures. From a thorough examination of the various pyrolysis steps, we developed a steam treatment for dried PZT gels ensuring decomposition to a homogeneous, amorphous oxide mixture Pb(Zr/Ti)O<sub>3</sub> at a temperature of about 300 °C.

## 2. Experimental procedure

PZT samples were prepared from Pb(Ac)<sub>2</sub>·3H<sub>2</sub>O, Zr(O<sup>n</sup>Pr)<sub>4</sub> and Ti(O<sup>n</sup>Pr)<sub>4</sub> dissolved in 2-methoxyethanol. After addition of 5 (PZT(0) = PT)–20 (PZT(100) = PZ) mol H<sub>2</sub>O per mol (Zr/Ti) the sol gelled in about 15 min. The gel was dried at 90 °C at a pressure of 20 mbar and crushed to a fine powder. Samples of Zr<sub>x</sub>Ti<sub>1-x</sub>O<sub>2</sub> [labelled ZT(*x*)] were prepared analogously without lead acetate and reduced amounts of water due to faster gelation. For steam treatment, the samples were placed in a small beaker, which stood in a larger, tightly closed vessel containing some water on the bottom. The vessel was kept for 6 h at 105 °C, so that the PZT sample was in contact with the water vapour, but not with liquid water.

Fourier transform Raman spectra were recorded in 180° reflection geometry with a Bruker RA 106 spectrometer using an excitation wavelength of 1064 nm.

A Netzsch STA 409 was used for simultaneous differential thermal analysis (DTA) and thermogravimetry (TGA). Some 10–50 mg of sample were

placed in an  $\text{Al}_2\text{O}_3$  crucible. For the DTA–TG–infrared (i.r.) measurements the reference crucible also contained sample material (but less than the sample crucible) to increase the total amount of sample material. The purge gas was  $0.21 \text{ min}^{-1}$  of dry air. The exhaust gas from the DTA furnace was transferred through a heated ( $140^\circ\text{C}$ ) steel tube into a heated ( $140^\circ\text{C}$ ) steel gas-flow-through cuvette with KBr windows. The heating rate for the i.r. coupling measurements was  $\alpha = 3.5 \text{ K min}^{-1}$ .

Fourier transform infrared (FTIR) spectra of the gaseous pyrolysis products were recorded with a Bruker IFS 66 spectrometer and Opus chrom 3D measuring software. Spectra were recorded in the range  $800\text{--}3600 \text{ cm}^{-1}$  with a resolution of  $2 \text{ cm}^{-1}$ . Measuring one spectrum takes about 22 s, which yields a resolution on the temperature scale of the DTA run of  $\approx 1 \text{ K}$ . The integrals of the i.r. absorbance peaks are proportional to the concentration of the substances in the exhaust gas. The proportionality constants were determined with calibration measurements. For reactions with only one gaseous product, the weight loss,  $dm/dt$ , of this substance can be calculated as the derivative of the TGA curve (DTGA), and related to the integrated peak intensities of the i.r. spectra. For the calibration of  $\text{H}_2\text{O}$  and  $\text{CO}_2$ , dehydration of  $\text{CuSO}_4 \cdot 5\text{H}_2\text{O}$  and decomposition of  $\text{PbCO}_3$  to  $\text{PbO}$  and  $\text{CO}_2$  were used. Acetone and acetic acid were evaporated directly from the DTA crucible. For water, the five integrals of the rotational bands are summed up. The integration for the organic compounds is performed in such ranges where the bands

do not overlap. The carbonyl stretching bands of acetone and acetic acid are not suitable for evaluation due to overlap with  $\text{H}_2\text{O}$  rotational bands. The choice of integration ranges and baselines is illustrated in Fig. 1.

Activation energies were determined from the shift of the DTA and DTGA peak maximum temperature,  $T_m$ , with increasing heating rates in the range  $1\text{--}30 \text{ K min}^{-1}$  according to Kissinger [11] and Graydon *et al.* [12] from a plot of  $\ln(\alpha/T_m^2)$  versus  $1/T_m$ .

### 3. Results and discussion

#### 3.1. Composition of the dried PZT gels

The major part of organic components in the dried PZT gels are the acetate groups incorporated from lead acetate. The high similarity of the i.r. spectra of the dried gels and lead acetate in the carbonyl stretching region [13] indicates that they are still bonded to  $\text{Pb}^{2+}$  in the dried gel. The Raman spectra of dried PZT (45) gel and anhydrous lead acetate (almost completely amorphous after removal of the crystal water from  $\text{Pb}(\text{Ac})_2 \cdot 3\text{H}_2\text{O}$  by evacuation), depicted in Fig. 2, also exhibit a high similarity. Nevertheless, small amounts of acetate groups could also be connected to zirconium or titanium. For this reason, the pyrolysis of zirconium and titanium acetates shall be examined, in addition to the pyrolysis of pure lead acetate and PZT gels.

For further comparison, the Raman spectrum of dried ZT(45) gel is presented in Fig. 2, which contains

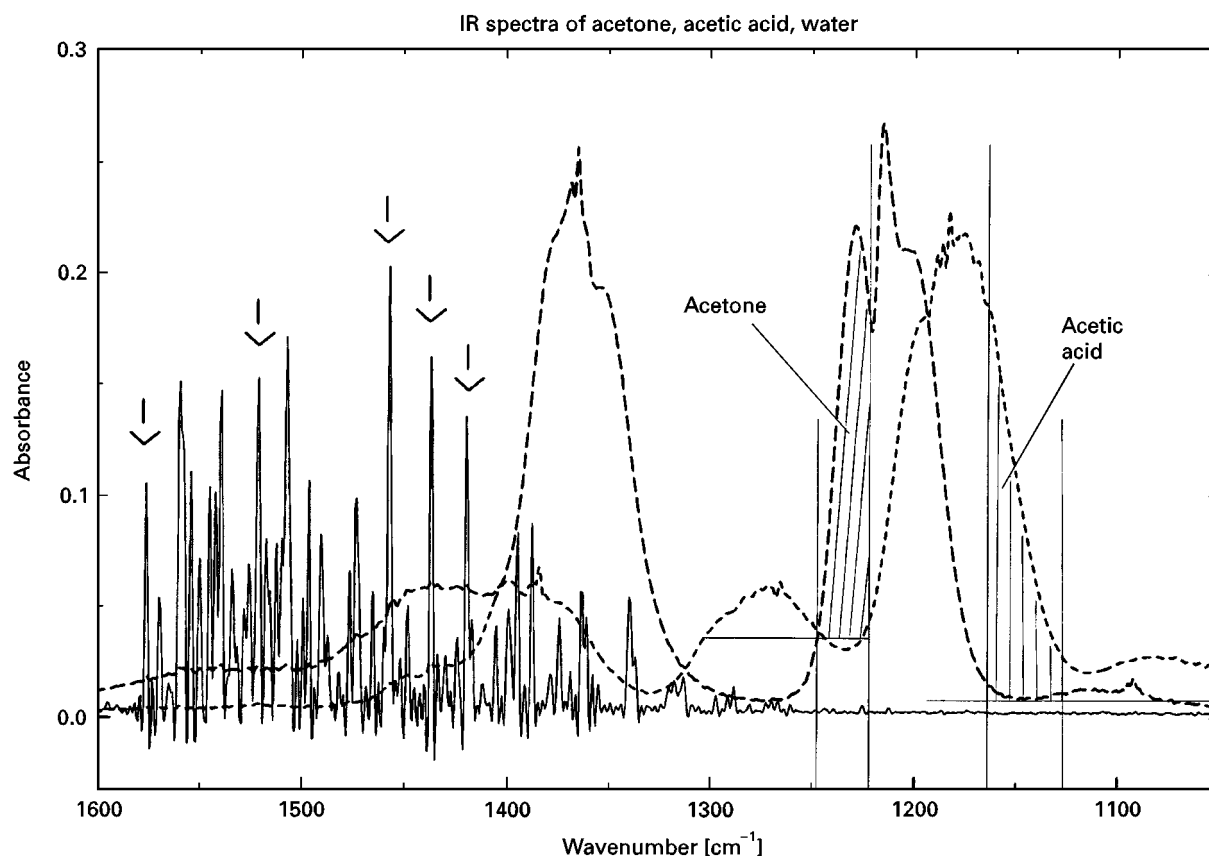


Figure 1 I.r. spectra of gaseous  $\text{H}_2\text{O}$ , acetone and acetic acid. Integration areas are hatched, the evaluated peaks of  $\text{H}_2\text{O}$  are marked with arrows: — acetone; --- acetic acid; — water.

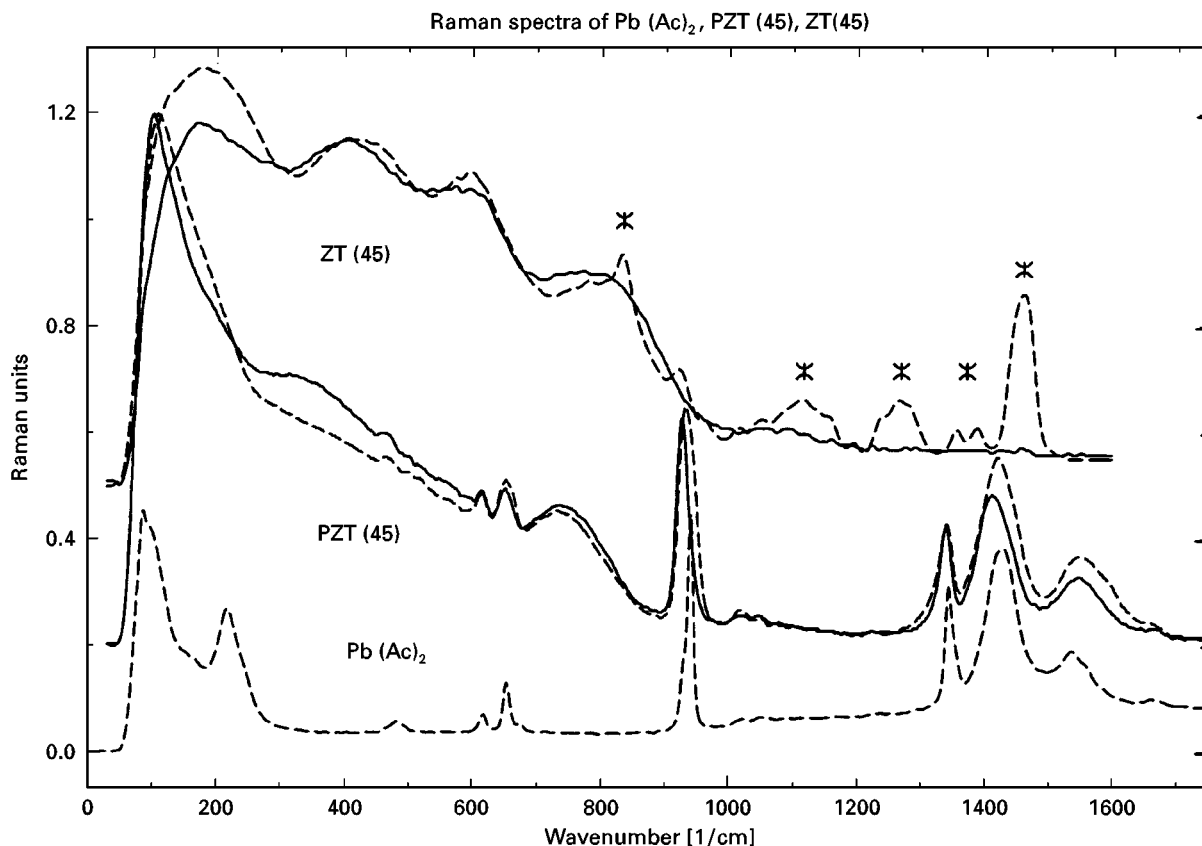


Figure 2 Raman spectra of anhydrous lead acetate and dried PZT(45), ZT(45) gels with and without steam treatment. The spectra are shifted along the ordinate for clarity, the asterisks mark the bands of methoxyethoxide groups: -- no steam treatment; — steam treatment.

residual methoxyethoxide groups (marked by asterisks). The lack of these bands in the PZT(45) spectra indicates almost complete hydrolysis of alkoxides during gelation of the dried PZT samples. Thus the composition of the dried PZT gels can be approximated by the formula  $\text{PbO}_{1-y}(\text{Ac})_{2y}(\text{Zr/Ti})\text{O}_2$ .

### 3.2. Pyrolysis of lead, zirconium and titanium acetate

The pyrolysis of pure lead, zirconium and titanium acetates is investigated prior to the more complex PZT gels. For pyrolysis of the carboxylates of earth alkali metals, Pb, Zn and Cd, the formation of  $\text{CO}_2$  and a symmetric ketone at pyrolysis temperatures of 200–400 °C is a well known reaction



Depending on the basicity of the metal oxide, a metal carbonate or a metal oxide is formed. A radical reaction mechanism is established for lead and calcium decanoate [14, 15]. For pyrolysis of the corresponding acetates, the same mechanism can be assumed.

The results of the DTA–TGA and i.r. measurements of lead acetate pyrolysis in air are shown in Fig. 3. Acetone,  $\text{CO}_2$ ,  $\text{H}_2\text{O}$  and minor amounts of acetic acid can be identified as gaseous pyrolysis products in the i.r. spectra. Immediately after the melting point of lead acetate at 204 °C, decomposition begins with the formation of acetone and  $\text{CO}_2$  in equimolar amounts. The weight loss calculated from the derivative of the TGA curve (DTGA) equals the weight loss calculated

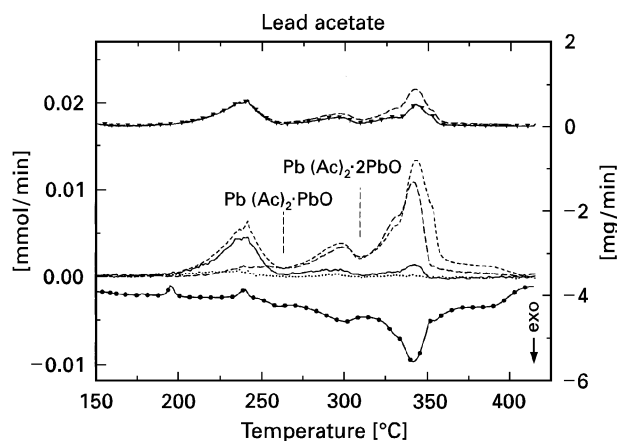


Figure 3 DTA–TGA–i.r. measurement of the pyrolysis of lead acetate,  $\alpha = 3.5 \text{ K min}^{-1}$ . Top: weight loss from TGA curve (DTGA) and from i.r. spectra ( $\text{dm i.r./dt}$ ); middle: flow of gaseous pyrolysis products from i.r. spectra; bottom: heat flow (DTA curve):  $\blacktriangledown$  DTGA; --  $\text{dm i.r./dt}$ ; — acetone; ... acetic acid; ---  $\text{CO}_2$ ; - -  $\text{H}_2\text{O}$ ;  $\bullet$  DTA.

from the integration of all peaks in the i.r. spectra. Acetone formation is slightly exothermic and continues up to 270 °C. At this temperature the solid residue has the composition of a lead subacetate  $\text{Pb}(\text{Ac})_2 \cdot \text{PbO}$ . In the next, slightly exothermic step, until 310 °C mainly  $\text{CO}_2$  and  $\text{H}_2\text{O}$  are formed by oxidation. At 310 °C, the solid residue has the composition of another lead subacetate  $\text{Pb}(\text{Ac})_2 \cdot 2\text{PbO}$ . At higher temperatures up to 350 °C, more  $\text{CO}_2$  and  $\text{H}_2\text{O}$  are formed in a strongly exothermic oxidation step.

At 350–415 °C, some CO<sub>2</sub> is liberated from PbCO<sub>3</sub> formed intermediately. During the oxidation steps the weight loss calculated from the i.r. spectra of the gaseous products is higher than the value from the DTGA curve, because oxygen used in the oxidation is incorporated in the gaseous products. The H:C ratio calculated from the amounts of all gaseous products from the i.r. spectra is 1.56 and close to the theoretical value of 1.50. The various pyrolysis steps are summarized in Fig. 4.

The activation energies for the various pyrolysis steps of lead acetate and lead decanoate were determined from a series of DTA runs with different heating rates. The results are collected in Table I, together with the standard deviation calculated from the linear regression of the Kissinger plot. The activation energy of the acetone formation of lead acetate can be evaluated only from the shift of the DTGA peak, because the DTA peak is too weak. The activation energy of 131 kJ mol<sup>-1</sup> agrees well with the value of 124 kJ mol<sup>-1</sup> reported in [16] for the decomposition of lead acetate in a nitrogen atmosphere. Thus the formation of acetone is independent of the atmosphere. The activation energies from the evaluation of the DTA and DTGA peaks of the oxidation at 290 °C coincide at about 160 kJ mol<sup>-1</sup>. The values of 218 (DTA) and 262 kJ mol<sup>-1</sup> (DTGA) for the oxidation step around 340 °C differ because of the retarded liberation of CO<sub>2</sub> from CO<sub>3</sub><sup>2-</sup>, which shifts the DTGA peak relative to the DTA peak.

The decomposition of lead decanoate Pb(Dec)<sub>2</sub> (melting point 99 °C) starts with the formation of nonadecanone and CO<sub>2</sub> at 200–310 °C in a slightly exothermic reaction. After this step, the solid residue has the composition of Pb(Dec)<sub>2</sub>·PbCO<sub>3</sub>. A strongly exothermic oxidation step occurs at 310–360 °C, yielding a solid residue of PbCO<sub>3</sub>·CO<sub>2</sub> liberation from PbCO<sub>3</sub> ends at 450 °C. The ketone formation activation energies of 138 (DTA) and 147 kJ mol<sup>-1</sup> (DTGA) are very similar to the values of acetone formation from lead acetate. This is a strong support for the assumption that acetone formation from lead acetate also occurs with a radicalic mechanism.

The results of the DTA–TGA i.r. measurements for zirconium acetate with heating rates of 3.5 and 15 K min<sup>-1</sup> are shown in Fig. 5. In contrast to the pyrolysis of lead acetate, acetic acid is the main organic decomposition product. It is formed by the hydrolysis of acetate groups with small amounts of water from oxidation processes. In the DTA run with α = 3.5 K min<sup>-1</sup>, acetic acid and small amounts of CO<sub>2</sub> from oxidation are formed at 170–260 °C in a slightly endothermic reaction. The solid residue has the composition ZrO(Ac)<sub>2</sub>. In the following step at about 300 °C, acetone and CO<sub>2</sub> are the main products. At 310–380 °C H<sub>2</sub>O and CO<sub>2</sub> are formed in an exothermic oxidation, leaving a solid residue of white ZrO<sub>2</sub>. The decomposition steps are different when a high heating rate of 15 K min<sup>-1</sup> is applied. The formation of a small amount of acetone occurs

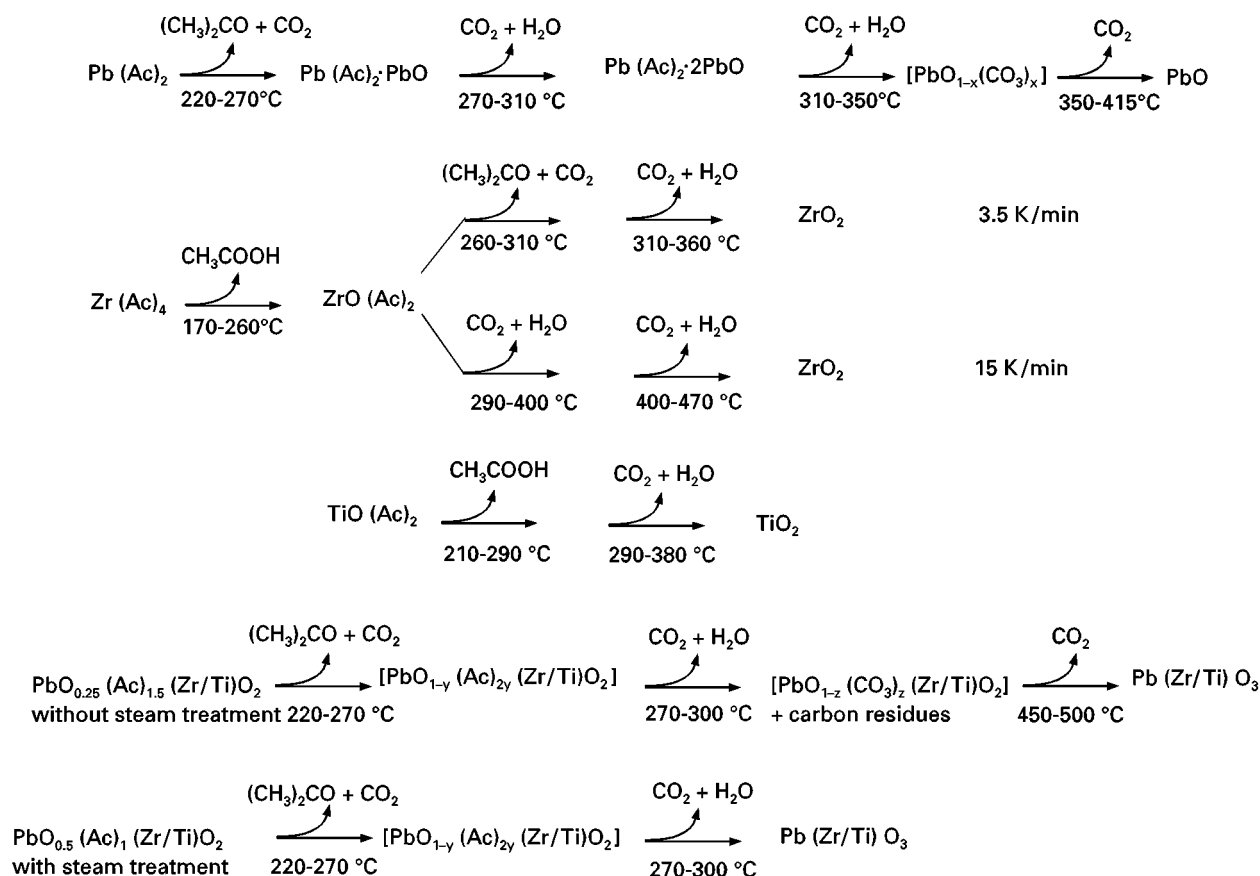


Figure 4 Summary of the various pyrolysis steps of lead, zirconium and titanyl acetate and PZT gels. Intermediates with variable stoichiometry are indicated by square brackets.

TABLE I Activation energies,  $E_a$  (with standard deviation from linear regression), for the pyrolysis of lead acetate, lead decanoate, zirconium acetate and titanyl acetate

	$E_a$ from DTA peak (kJ mol <sup>-1</sup> ) <sup>a</sup>	$E_a$ from DTG peak (kJ mol <sup>-1</sup> ) <sup>a</sup>
Pb(Ac) <sub>2</sub>		
Acetone formation at 200–270 °C		131 ± 2(3)
Oxidation		
At 270–310 °C	155 ± 3(2)	165 ± 5(3)
At 310–350 °C	218 ± 6(3)	262 ± 7(3)
Pb(Dec) <sub>2</sub>		
Ketone formation at 200–310 °C	138 ± 3(2)	147 ± 4(3)
Oxidation at 310–360 °C	308 ± 35(11)	264 ± 19(7)
Zr(Ac) <sub>4</sub> <sup>b</sup>		
Acetic acid		
At 170–210 °C, <b>1</b>		201 ± 19(10)
At 210–260 °C, <b>2</b>		141 ± 5(3)
Low heating rates, 1–5 K min <sup>-1</sup>		
Acetone formation at 280–310 °C, <b>3</b>		133 ± 9(7)
Oxidation at 310–370 °C, <b>4</b>	142 ± 3(2)	
High heating rates, 10–30 K min <sup>-1</sup>		
Oxidation at 310–390 °C, <b>5</b>		261 ± 31(12)
Oxidation at 390–480 °C, <b>6, 7</b>	44 ± 4(9)	73 ± 7(9)
TiO(Ac) <sub>2</sub>		
Acetic acid at 220–290 °C		255 ± 11(4)
Oxidation at 290–380 °C	167 ± 3(2)	188 ± 6(3)

<sup>a</sup> Values in parentheses are percentages.

<sup>b</sup> Numbers in bold indicate order of pyrolysis steps, which are shown in Fig. 6.

together with the formation of acetic acid and CO<sub>2</sub> at 170–290 °C. Up to 400 °C, H<sub>2</sub>O and CO<sub>2</sub> are produced in a slightly exothermic reaction, followed by strongly exothermic oxidation at 400–470 °C. The solid residue of ZrO<sub>2</sub> is still grey at 600 °C, containing some carbon residues.

According to the change of the decomposition process with the heating rate, the Kissinger plot of  $\ln(\alpha/T_m^2)$  versus  $1/T_m$  shown in Fig. 6 exhibits different straight lines at low and at high heating rates. Only the formation of acetic acid at about 190 and 230 °C yields single lines for all heating rates. The activation energies for zirconium acetate are also collected in Table I. The activation energy of acetone formation is similar to the value found for lead acetate, but the temperature of acetone formation is higher. The yield of acetone from zirconium acetate (18% for  $\alpha = 3.5$  K min<sup>-1</sup> and 12% for  $\alpha = 15$  K min<sup>-1</sup>) is much lower than the yield found for lead acetate (50%).

Titanium tetraacetate Ti(Ac)<sub>4</sub> is not a stable compound, thus only titanyl acetate TiO(Ac)<sub>2</sub> can be examined. Acetic acid, H<sub>2</sub>O and CO<sub>2</sub> are the main products during the pyrolysis of TiO(Ac)<sub>2</sub>. Bands of some unknown organic components overlap with the other bands in the i.r. spectra and make the integration impossible. In a first step at 220–290 °C, acetic acid is the main product. Exothermic oxidation pro-

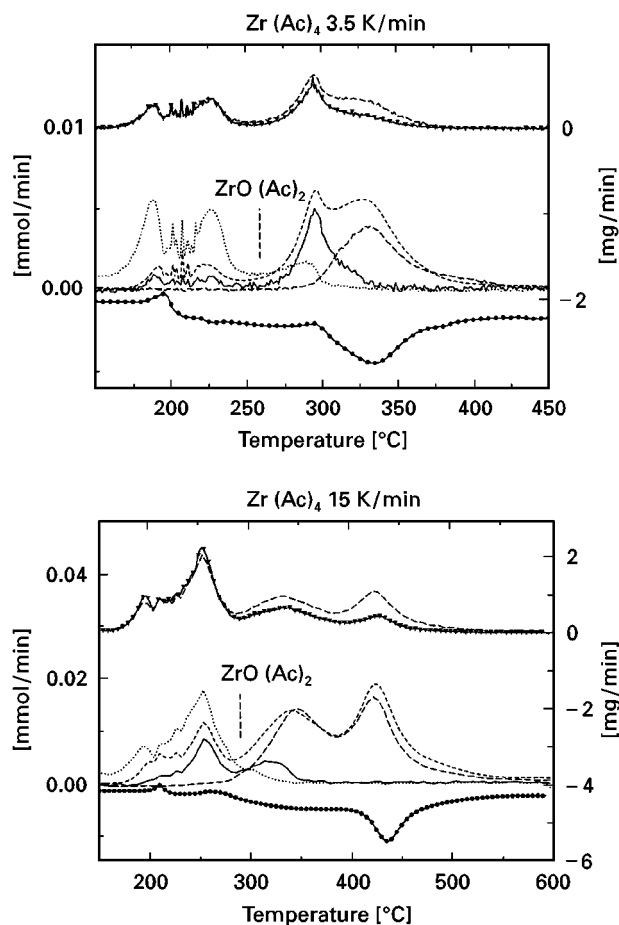


Figure 5 DTA-TGA-i.r. measurements of pyrolysis of zirconium acetate with heating rates of 3.5 and 15 K min<sup>-1</sup>: ▼ DTGA; — dm<sub>i.r.</sub>/dt; — acetone; ... acetic acid; --- CO<sub>2</sub>; -·- H<sub>2</sub>O; ● DTA.

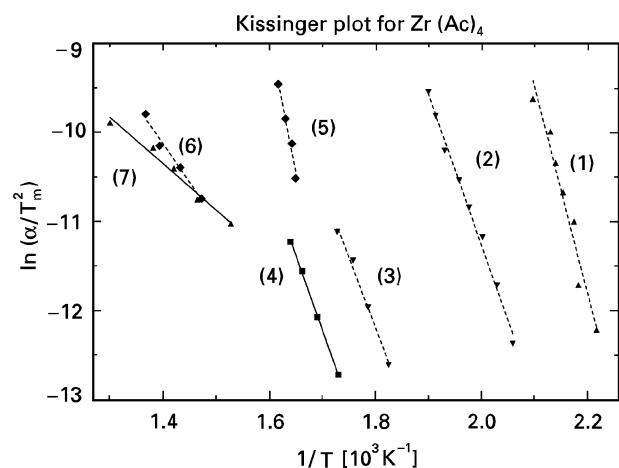


Figure 6 Kissinger plot for the pyrolysis of zirconium acetate. The labels correspond to the pyrolysis steps listed in Table I: — DTA peaks; --- DTGA peaks.

ducing H<sub>2</sub>O and CO<sub>2</sub> follows at 290–380 °C. The residue is white TiO<sub>2</sub>. These pyrolysis steps do not change when the heating rate is varied. The activation energies of these steps are also contained in Table I. The pyrolysis of zirconium and titanyl acetate with acetic acid as the main product is clearly different from the pyrolysis of lead acetate.

### 3.3. Pyrolysis of PZT gels

The DTA–TGA–i.r. measurements of PT and PZT(45) gels without steam treatment are shown in Fig. 7. The total weight loss of about 18% corresponds to a dried gel composition of approximately  $\text{PbO}_{0.25}(\text{Ac})_{1.5}(\text{Zr/Ti})\text{O}_2$ . It is known that the volatile ester methoxyethanol-acetate is formed in solutions containing lead acetate, (Zr/Ti) alkoxides and methoxyethanol [8], so that a part of the acetate group is lost. The pyrolysis starts with the formation of acetone,  $\text{CO}_2$  and small amounts of acetic acid. The yield of acetone is about 0.35 mol per mol of PZT gel, i.e. 47% of the theoretical yield from the amount of acetate groups present in the gels. This step shows no DTA signal. At 250–300 °C, an exothermic oxidation step follows, producing mainly  $\text{CO}_2$  and  $\text{H}_2\text{O}$ . After this step the samples are black. At 450–500 °C, these samples show an additional weight loss of 3–4%, and mainly  $\text{CO}_2$  is set free. This step is more (PZT(45)) or less (PT) exothermic. Afterwards, the samples are pale yellow (PT) or dark yellow (PZT(45)). The small DTA crystallization peaks are superimposed by stronger DTA peaks related to weight loss.  $\text{CO}_2$  can originate from the carbon residues in a strongly exothermic reaction, or from  $\text{PbCO}_3$  with little heat production. I.r. spectra of the solid residues heated to temperatures above 300 °C show peaks of internal  $\text{CO}_3^{2-}$  vibrations. A part of the  $\text{CO}_2$  produced in the oxidation step from 250 to 300 °C is bonded to  $\text{PbO}$ , forming  $\text{PbCO}_3$ . The

amount of  $\text{CO}_3^{2-}$  detected in the i.r. spectra increases from 300 to 450 °C due to slow oxidation of carbon residues. Assuming that the carbon atoms contained in the samples above 300 °C are either elementary carbon or bound in carbonate groups, the amount of each of these species can be calculated from comparison of the DTGA weight loss ( $-\text{CO}_2$  from  $\text{PbCO}_3$  and  $-\text{C}$  from carbon residues) with the amount of  $\text{CO}_2$  found in the exhaust gas. We find about 0.13 mmol  $\text{PbCO}_3$  and 0.13 mmol carbon residues per mmol PT dried gel, and about 0.20 mmol  $\text{PbCO}_3$  and 0.33 mmol carbon residues per mol PZT(45) gel. The pyrolysis steps identified for PZT gels are also contained in Fig. 4.

The DTA–TGA–i.r. measurements of dried PT and PZT(45) gel after steam treatment are shown in Fig. 8. The total weight loss of these PT and PZT(45) samples is about 14%, which corresponds to a dried gel composition of  $\text{PbO}_{0.5}\text{Ac}(\text{Zr/Ti})\text{O}_2$ . The course of the decomposition of the organic components is very similar for both samples. Pyrolysis begins with the formation of about equimolar amounts of acetone and  $\text{CO}_2$  at 200–270 °C. The yield of acetone is about 0.2 mol per mol PZT gel, i.e. 40% of the theoretical yield from the amount of acetate groups contained in the gel. At 250–300 °C,  $\text{H}_2\text{O}$  and  $\text{CO}_2$  are formed in a strongly exothermic oxidation step. No further weight loss occurs at higher temperatures. The solid residue is pale yellow. These samples are pyrolysed without

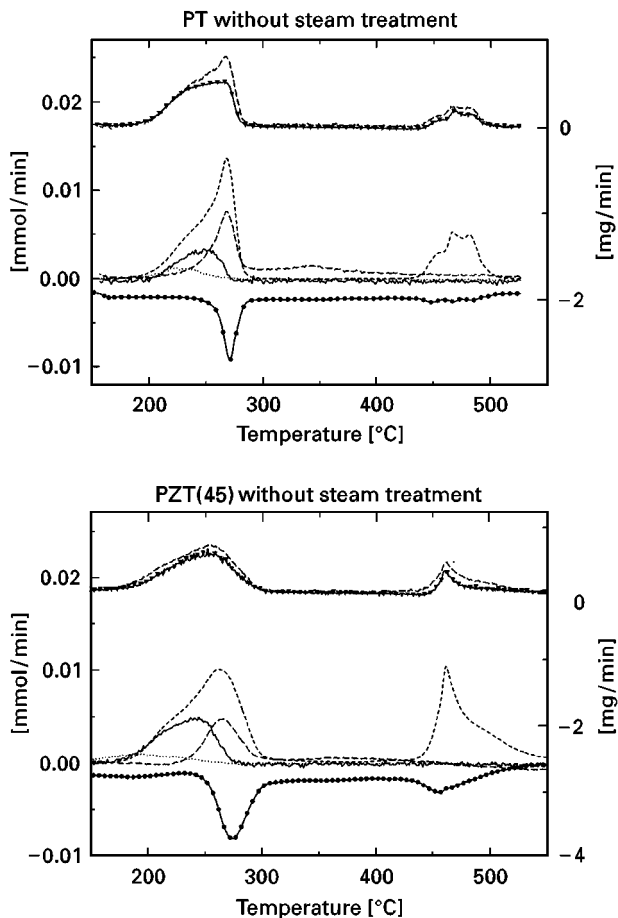


Figure 7 DTA–TGA–i.r. measurements of the pyrolysis of dried PT and PZT (45) gels without steam treatment,  $\alpha = 3.5 \text{ K min}^{-1}$ : ▼ DTGA; --  $\text{dm}_{\text{i.r.}}/\text{dt}$ ; — acetone; ... acetic acid; ---  $\text{CO}_2$ ; --  $\text{H}_2\text{O}$ ; ● DTA.

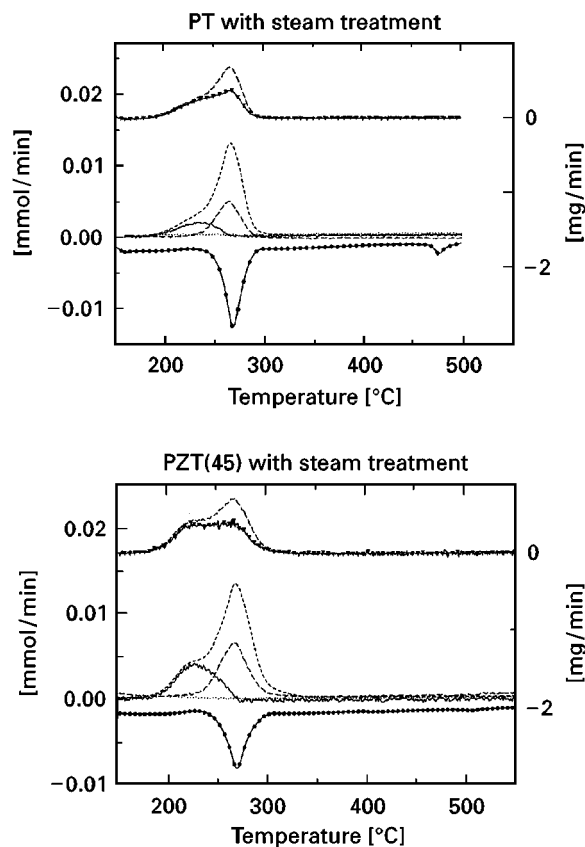


Figure 8 DTA–TGA–i.r. measurements of the pyrolysis of dried PT and PZT(45) gels with steam treatment,  $\alpha = 3.5 \text{ K min}^{-1}$ : ▼ DTGA; --  $\text{dm}_{\text{i.r.}}/\text{dt}$ ; — acetone; ... acetic acid; ---  $\text{CO}_2$ ; --  $\text{H}_2\text{O}$ ; ● DTA.

TABLE II Activation energies,  $E_a$  (with standard deviation from linear regression), for the decomposition of organic residues of PT–PZ gels with steam treatment<sup>a</sup>

Sample	$E_a$ from DTGA peak (kJ mol <sup>-1</sup> )	$E_a$ from DTA peak (kJ mol <sup>-1</sup> )	$E_a$ from DTGA peak (kJ mol <sup>-1</sup> )	$E_a$ from DTA peak (kJ mol <sup>-1</sup> )
	Acetone formation	Oxidation	Oxidation of carbon residues	
PT	113 ± 5(5)	134 ± 5(4)		
PZT(10)	126 ± 5(4)	128 ± 8(6)		
PZT(25)	121 ± 3(2)	137 ± 7(5)		
PZT(35)	125 ± 8(7)	145 ± 4(3)		
PZT(45)	116 ± 5(5)	151 ± 5(3)		
PZT(75)	144 ± 4(3)	124 ± 3(2)	399 ± 15(4)	499 ± 37(7)
PZ	162 ± 8(5)	130 ± 3(3)	263 ± 16(6)	404 ± 28(7)

<sup>a</sup>Values in parentheses are percentages.

formation of carbon residues. PT shows a small exothermic crystallization peak at 480 °C. The crystallization of PZT(45) is less exothermic and occurs at higher temperatures.

In Table II the activation energies of the pyrolysis steps of various samples, PT–PZ, after steam treatment are collected. The activation energy of the oxidation step can be evaluated directly from the exothermic DTA peak. The DTGA peak of acetone formation overlaps with the weight loss due to oxidation at somewhat higher temperatures. The DTA oxidation peak can be scaled in such a way that it is in good coincidence with the DTGA peak at about 260–300 °C. Subtraction of this curve from the DTGA peak leaves only that part of the DTGA peak caused by acetone formation at lower temperatures. From the  $T_m$  shift of these curves with heating rate the activation energy of acetone formation was evaluated. For PZT(75) and PZ oxidation occurs at higher temperatures, causing only a shoulder on the DTGA acetone formation peak. These DTGA peaks can be evaluated directly for calculation of the activation energy of acetone formation.

The temperature range, the activation energy and the yield of acetone from PZT gels are very similar to those of lead acetate. This is a clear indication that most of the acetate groups in the gel are bonded to Pb<sup>2+</sup>. The activation energy of the oxidation step of the PZT gels is also similar to that of the first oxidation step of lead acetate, but in PZT gels pyrolysis is completed with this oxidation up to 300 °C, and for lead acetate a second oxidation step follows at higher temperatures. This shows that (Zr/Ti) atoms have some influence on pyrolysis at higher temperatures.

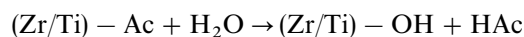
PZT gels with more than 52% zirconium contents are pyrolysed with the intermediate formation of carbon residues and small amounts of PbCO<sub>3</sub>, leading to an exothermic weight loss at 450–500 °C, even after steam treatment. The results of DTA–TGA–i.r. measurements resemble those of PZT(45) without steam treatment. The activation energies of acetone formation and oxidation are similar to the activation energies for the titanium-rich samples. The activation energies of the decomposition step at 450–500 °C are different for the DTA and DTGA peaks and vary with sample composition.

### 3.4. Reasons for the formation of carbon residues

Comparison with pyrolysis behaviour of other samples prepared by the sol-gel process gives insight into the reasons for the formation of carbon residues. Without preceding steam treatment, samples of ZT(x) form carbon residues from residual methoxyethoxide groups during pyrolysis. Steam treatment removes all the methoxyethoxide groups, which can be recognized by disappearance of corresponding bands in Fig. 1, and prevents the formation of carbon residues. This leads to the conclusion that in zirconium-rich PZT gels after steam treatment the acetate groups must be the starting material for the formation of carbon residues.

Lead acetate and titanyl acetate are pyrolysed without carbon residues. In the PZT series, a problem arises with growing zirconium content. This indicates that acetate groups bonded to zirconium are the reason for the carbon residues. Although most of the acetate groups are bonded to lead, a small amount bonded to zirconium can be sufficient to cause black coloration of the samples. Pyrolysis of zirconium acetate at high heating rates also shows the formation of residues, which are decomposed only at temperatures above 400 °C.

An examination of the water in the vessel used for steam treatment shows a decrease of pH from 5.5 before to 3.5–3.8 after treatment. I.r. spectra of the water exhibit weak bands of acetic acid, formed in the reaction



In zirconium-poor PZT gels, the few acetate groups bonded to zirconium are removed by steam treatment, and the samples can be pyrolysed without carbon residues. In zirconium-rich samples, too many zirconium bonded acetate groups are present and cannot be removed even with repeated steam treatment. The newly formed (Zr/Ti)-OH groups are acidic and can prevent the formation of PbCO<sub>3</sub> in steam treated PZT gels. The Raman spectra of PZT(45) and ZT(45) contained in Fig. 1 show a slight modification in the low wave-number region due to steam treatment, which could be caused by rearrangements in the amorphous (Zr/Ti) O<sub>6</sub> octahedra network.

#### 4. Conclusions

The pyrolysis of PZT gels synthesized from (Zr/Ti) alkoxides and lead acetate in methoxyethanol was investigated. The first pyrolysis step is similar to the first step in the pyrolysis of lead acetate, yielding acetone and CO<sub>2</sub>. This indicates that the major part of acetate groups is bonded to Pb<sup>2+</sup>. The oxidation that follows removes most of the organic components. Samples without steam treatment show the formation of undesired carbon and carbonate residues during pyrolysis. Steam treatment of the dried gels removes all residual alkoxide groups and part of the acetate groups bonded to titanium or zirconium. After this treatment, gels with up to 52% zirconium content pyrolyse without carbon and carbonate residues. These samples are suitable for further studies of crystallization kinetics. In the samples containing more than 52% zirconium, the formation of carbon residues, in spite of steam treatment, can be attributed to acetate groups still bonded to zirconium.

#### References

1. J. FUKUSHIMA, K. KODAIRA and T. MATUSHITA, *J. Mater. Sci.* **19** (1984) 595.
2. S. R. GURKOVICH and J. B. BLUM, in "Ultrastructure Processing of Ceramics, Glasses and Composites", edited by

- L. L. HENCH and D. R. ULRICH (Wiley, New York, 1984) p. 152.
3. J. B. BLUM and S. R. GURKOVICH, *J. Mater. Sci.* **20** (1985) 4479.
4. K. D. BUDD, S. K. DEY and D. A. PAYNE, *Proc. Brit. Ceram. Soc.* **36** (1985) 107.
5. C. LEMOINE, B. GILBERT, B. MICHAUX, J.-P. PIRARD and A. J. LECLoux, *J. Non-Cryst. Solids* **175** (1994) 1.
6. U. SELVARAJ, A. V. PRASADERO, S. KOMARNENI, K. BROOKS and S. KURTZ, *J. Mater. Res.* **7** (1992) 992.
7. M. KLEE, E. EUSEMANN, R. WASER, W. BRAND and H. VAN HAL, *J. Appl. Phys.* **72** (1002) 1566.
8. S. LI, R. A. CONDRATE and R. M. SPRIGGS, *J. Can. Ceram. Soc.* **57** (1988) 61.
9. A. D. POLLI and F. F. LANGE, *J. Amer. Ceram. Soc.* **78** (1995) 3401.
10. C. D. E. LAKEMAN and D. A. PAYNE, *ibid.* **75** (1992) 3091.
11. H. E. KISSINGER, *Anal. Chem.* **29** (1957) 1703.
12. J. W. GRAYDON, S. J. THORPE and D. W. KIRK, *Acta Metall. Mater.* **42** (1994) 3163.
13. D. GUTWERK, Dissertation, Universität Stuttgart (1995).
14. R. A. HITES and K. BIEMANN, *J. Amer. Chem. Soc.* **94** (1972) 5772.
15. H. A. ELLIS and E. K. OKOH, *J. Chem. Soc. Perkin Trans.* **1982** (1982) 1497.
16. M. A. MOHAMED, S. A. HALAWY and M. M. EBRAHIM, *Thermochim. Acta* **236** (1994) 249.

Received 26 January  
and accepted 30 June 1998